Transactions of the **14th International Conference on Structural Mechanics in Reactor Technology** (SMiRT 14), Lyon, France, August 17-22, 1997

HKW/11

Study on the dynamic inelastic behavior of seismic shear walls of the reactor building

Minami T.[(1)], **Nishikawa T.**[(2)], **Yoshimura M.**[(2)], **Ono H.**[(1)]
(1) Taisei Corporation, Japan
(2) Tokyo Metropolitan University, Japan

ABSTRACT : It is important to predict dynamic inelastic behavior of seismic shear walls to carry out reliable seismic design of nuclear power plant building. In 1996, SSWISP (Seismic Shear Wall International Standard Problem) conducted by NUPEC (Nuclear Power Engineering Corporation) was held, and its objective was to improve the analytical technique of seismic response of reactor buildings. We participated SSWISP and could confirmed our proposed method can predict the inelastic behavior of shear wall well.

1. INTRODUCTION

The details of SSWISP and test were mentioned in Ref.[1] and Ref.[2]. In simulating the offering problem, we used the analytical method as to be able to estimate dynamic inelastic response of seismic shear wall and as to apply for the design. We used the original method that was combined with static analysis using FEM model and dynamic analysis using Lumped-mass model. The analysis was carried out by 3-steps. In step-1, static monotonic loading analysis carried out by using the FEM model and the load-displacement relation was obtained. In step-2, non-linear load-displacement relation calculated from previous step was approximated to the multi-linear skeleton curve for the nonlinear analysis. In step-3, the dynamic behavior of the specimen was simulated by using the one lumped-mass model.

2. FEM MODEL ANALYSIS (STEP-1)

(1) Analytical Model

Fig-1 illustrates an outline of the FEM model used in the analysis. The 8-node isoparametric shell elements are used to express behavior of concrete and rebars. The 2-node joint truss elements are used to express pulling out behavior of the rebars from basemat. Linear shell elements are used for the top slab. Number of nodes is 111 and number of elements is 91 in the model. Pre-analysis to investigate the relation between mesh size and the analytical result was carried out, and it was confirmed that the mesh size had little influence on the analytical result.

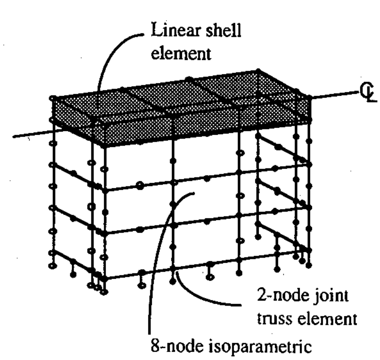

Fig.-1 FEM model

(2) Constitutive law of concrete

Bacicaly, SI-unit is used in this paper. Stress-strain relationship of concrete used in this analysis is shown in Fig-2. (Ref.[3]) Compressive stress-strain diagram under plane stress is formulated based on equivalent uniaxial stress-strain relation, taking account of the theory of orthotropic hypoelastic model. The yield envelope of concrete under plane stress is expressed by revised failure envelope suggested by Kupfer et.al.(Ref.[4]). In compressive region of this relationship, compressive strength is reduced at the generation of tensile crack. This phenomenon is expressed by using factor λ . The factor λ, expressed as follow Eq.-(1) is defined as a function of strain normal to crack (ε ct), and the maximum compressive stress (fc) and strain (ε c0) at the fc is regarded as constant . Not only compressive strength but also strain at the maximum strength is reduced simultaneously by factor λ . In this Fig-3, vertical axis represents factor λ and horizontal axis represents the ratio of the ε ct to ε c0.

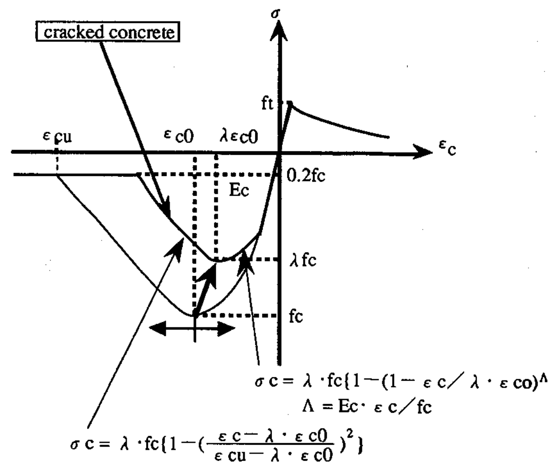

Fig.-2 Stress-strain relationship of concrete

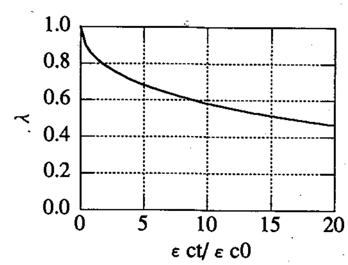

Fig.-3 Relationship of compressive strength reduction factor and strain ratio normal to crack.

$$\lambda = \exp(-0.2(\varepsilon ct / \varepsilon c0)^{1/2} \cdot kfc) \quad \cdot\cdot (1)$$

where, $kfc = 0.12fc^{2/3}$

Cracking stress under plane stress is formulated by the compressive strength, based on the experimental studies on reinforced concrete panels under pure shear. The equation is shown below.

$$ft = (0.068\text{-}fc/2500)\cdot fc \quad \cdot\cdot\cdot\cdot\cdot\cdot (2)$$

Tension stiffening model is formulated like following Eq.-(3) and Eq.-(4) by the concrete compressive strength, and bond characteristics due to crack direction and rebar direction. Smeared crack model is adopted for crack model.

$$\sigma cr = ft\,(\varepsilon cr / \varepsilon ct)^{c} \quad \cdot\cdot\cdot\cdot\cdot\cdot\cdot (3)$$

$$c = 0.023fc^{2/3}\,(\theta / 90)^{-1/2} \quad \cdot\cdot\cdot (4)$$

where ε ct : strain normal to crack

ε cr : cracking strain

θ : angle between crack and rebar

The shear transfer mechanism is expressed by using contact density model of cracked concrete, which is based on Li and Maekawas' model. (Ref.[5])

(3) Constitutive law of rebar

Average stress - average strain relationship of rebar embedded in concrete are modeled by a trilinear envelope curve as shown in Fig-4. The stress-strain relation of rebar embedded in concrete becomes inelastic as soon as rebar stress at a crack plane yield, and average stress of rebar embedded is smaller than that of bare bar. In the analysis, this phenomenon is expressed by using reduction factor α. The reduction factor α is fixed to 0.9, considering the reinforcement ratio of the wall and crack spacing in the test. The parameter ε_{st} is the strain at the start of strain hardening.

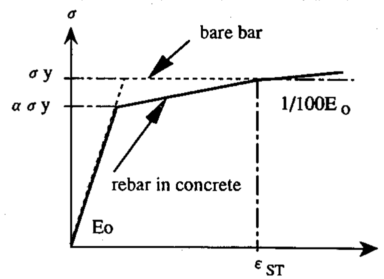

Fig.-4 Ave. stress - ave. strain relationship of bar in concrete.

(4) Slip model of embedded rebar

A pulling out displacement of rebar from basemat is modeled by the vertical spring element. The stress of this element represent the vertical rebar stress at the bottom of the wall, and the displacement represent the pulling out displacement from basemat. The relationship between rebar stress and pulling out displacement is consist of three zones according to inelastic condition at the bottom of the wall, and as shown in Fig.-5. Zone-1 is considered to be elastic region before cracking, zone-2 to be elastic region of rebar stress at the lower end of the wall, and zone-3 to be the region that rebar stress exceeds yield strength. In zone 2, rebar stress - pulling out displacement relationship is formulated like as Eq.-(5).

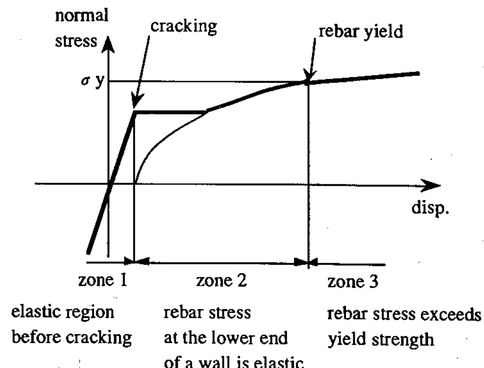

Fig.-5 Normal stress - disp. relationship of joint element represent a pulling out disp. of rebar from basemat.

$$\sigma_s = \{(165 \cdot \psi \cdot E^{0.5} \cdot \delta_{slip}) / A_s\}^{2/3} \quad \cdots \quad (5)$$

where, σ_s : rebar stress at the lower end of the wall

A_s : sectional area of rebar

ψ : perimeter length

E : modulus of elasticity

δ_{slip} : pulling out displacement of rebar

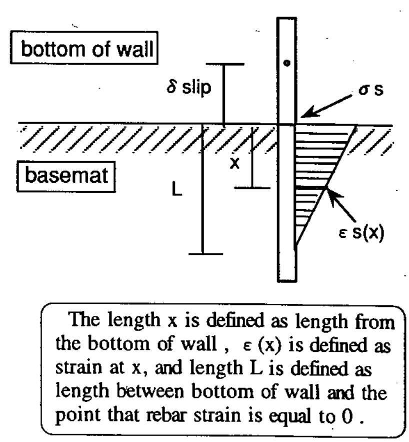

Fig.-6 Modeling pull out behavior

This equation was derived from the experimental equation as following Eq.-(6) for the relationship between the average bond stress on embedded part of rebar and the strain at the bottom end of the wall. (Ref.[6])

$$\tau = 82.4\sqrt{\varepsilon_s} \quad \cdots\cdots \quad (6)$$

where, τ : average bond stress on embedded part of rebar

ε_s : rebar strain at the bottom end of a wall

Strain distribution of tensile rebar in concrete is assumed to be a triangle like as Fig-6. As shown in Eq.-(7), δ slip is expressed by integrating the strain.

$$\delta_{slip} = \int_0^L \varepsilon_s(x)\,dx \quad \cdots (7)$$

(5) Result of FEM analysis

The analysis was carried out by displacement control. The analytical result on load-displacement relation is shown in Fig-7, together with the test result. The analytical result shows the good agreement with the test result.

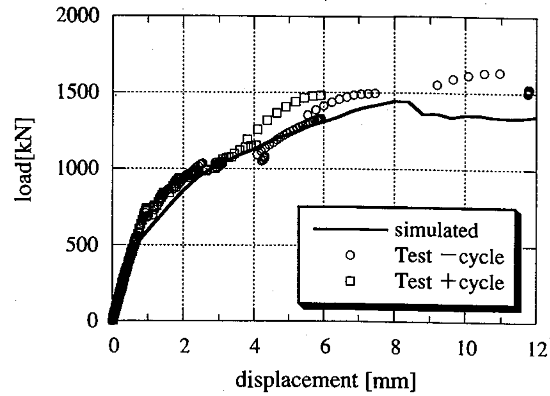

Fig.-7 FEM analytical result

3. MODELING LOAD-DIPLACEMENT RELATIONSHIP (STEP-2)

(1) Separating total displacement

First, the total displacement calculated from FEM analysis was separated into the flexural displacement and shear displacement. Flexural displacement was calculated from the vertical displacement of the flange wall in the FEM analysis, and displacement was separated using following procedure.

$$\delta f = \sum_{i=1}^{n} \left(hi \left(\phi i \cdot \Delta Xi \right) \right)$$

$$\phi i = (XLi - XRi)/(L0 \cdot \Delta Xi)$$

$$\delta s = \delta 0 - \delta f$$

where,

$\delta 0$: total displacement
δs : shear displacement
δf : flexural displacement

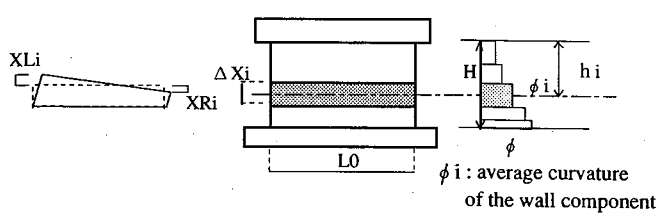

(2) Approximation of skeleton curve

Separated load-displacement relation was simplified for the nonlinear analysis as multi-linear envelope curve. Flexural relation was simplified as tri-linear, and shear relation was simplified as multi-linear which has negative gradient after the maximum strength. As for the method of modeling, the breaking point was defined where a big stiffness change occured in the skeleton, and each point was joined by straight line. Fig.-9 and Table-1 show each skeleton.

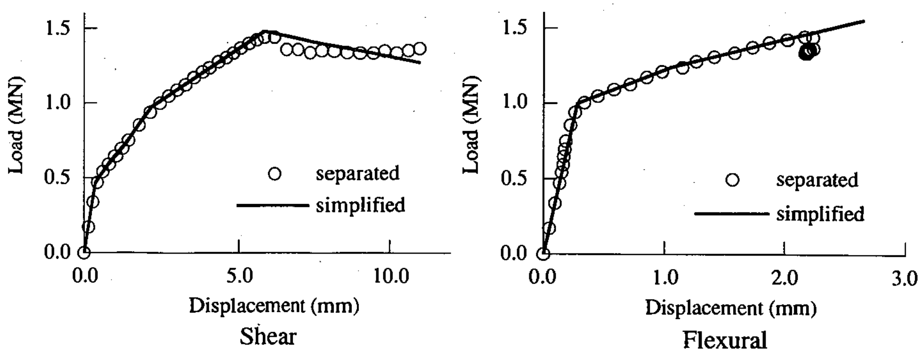

Fig.-9 Approximated skeleton curves used for dynamic analysis

Table-1 Braking point of skeleton curves

Shear				Flexural		
	1 st	2 nd	3 rd		1 st	2 nd
Q (kN)	462.1	915.6	1481.2	Q (kN)	994.4	1235.6
disp. (mm)	0.4	2.2	5.84	disp. (mm)	0.28	1.06
reduction ratio of stiffness *1	0.247	0.121	-0.036	reduction ratio of stiffness *1	0.088	0.057

*1) It means a ratio to the initial stiffness.

4. DINAMIC RESPONSE ANALYSIS (STEP-3)

(1) Analytical Model

The model for the dynamic response analysis is a base-fixed one lumped-mass model as shown in Fig.-10. The lumped-mass is placed at the center of the top slab, and the wall between the top of the base slab to the bottom of the top slab is replaced to a massless spring element that has shear and flexural stiffness and damping. The lower half of the top slab is modeled as a rigid beam. The mass and rotational moment of inertia of the lumped-mass are regarded at lumped-mass, that were calculated taking account of the top slab, additional weight and upper half of the wall. The initial stiffnesses of flexural and shear were determind from stiffness between the origin and first breaking point of skeleton. The constants of model are shown in Table-2.

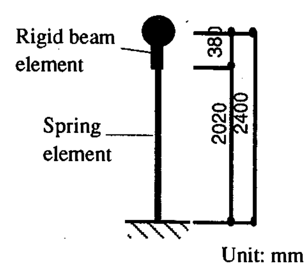

Fig.-10 Lumped-mass model

Table-2 Constants of dynamic analytical model

mass	mass: W (kg)	1.22×10^{3}
	rotational moment of inertia: I0 (kg/mm^2)	1.63×10^{13}
spring	sectional area: As (mm^2)	2.25×10^{5}
	shear modulus: G (MPa)	8.59×10^{3}
	Young's modulous: E (MPa)	2.29×10^{4}
	moment of inertia of area: I (mm^4)	1.45×10^{12}

(2) Hysteresis loop of spring

Hysteresis loops of shear and flexural springs are assumed as Fig-11. In these models, equivalent viscous damping is constant in stable loops. Shear hysteresis loop has slip component and negative gradient after maximum strength.

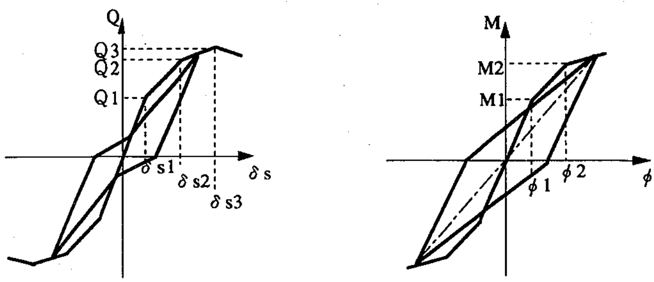

Shear Flexural

Fig.-11 Hysteresis loops of each spring

(3) Evaluation of damping

Two kinds of damping, viscous and hysteresis damping, were taken into account in the spring. Viscous damping is in proportion to initial stiffness and the value is 0.8% of critical which was calculated from the transfer function in the elastic response of RUN-1 and is assumed to be constant. Hysteresis damping factor is assumed in the manner that the sum of the hysteresis damping and viscous damping (0.8%) is equal to the equivalent viscous damping values obtained from the load-displacement relations in each RUN in the test. The same values were used both in shear and flexure. The damping values are shown in Table-3.

Table-3 Damping factor used for dynamic analysis

	RUN-1	RUN-2	RUN-2'	RUN-3	RUN-4	RUN-5
Total damping (%)	0.8	0.8	0.8	3.0	3.5	5.0
viscous damping (%)	0.8	0.8	0.8	0.8	0.8	0.8
hysteretic danping (%)	0.0	0.0	0.0	2.2	2.7	4.2

(4) Evaluation of stiffness reduction caused by a previous RUN

In the test, the input wave from RUN-1 through RUN-5 were sequentially applied to the specimen, using the same artificial waves with increasing accelerations. In the analysis, the deterioration of stiffness caused by the previous RUN has to be taken into account. It was confirmed by the pre-analysis that input of the previous just one wave was enough for taking account of the influence of stiffness degradation. Therefore, in this analysis, two waves (the waves for the previous RUN and the objective RUN) were input successively to calculate the response in each objective RUN.

5. ANALYTICAL RESULT

The analytical results of RUN-4 where observed maximum shear deformation angle was about 2/1000 and of RUN-5 where failure was occurred. Time history of horizontal acceleration and displacement response at the top slab are shown in Fig.-12 and Fig.-13, together with the test results. Inelastic response before failure at the test can be simulated well. As for the RUN-5, occurrence time of failure is simulated well, and analytical response after the occurrence of failure diverged.

Fig.-14 shows the envelope curves, which draw the renewing point of displacement or inertia-force in each RUN. In case of RUN-4, analytical result shows the good agreement with the test results. In case of RUN-5, negative gradient of skeleton can be expressed in the analysis.

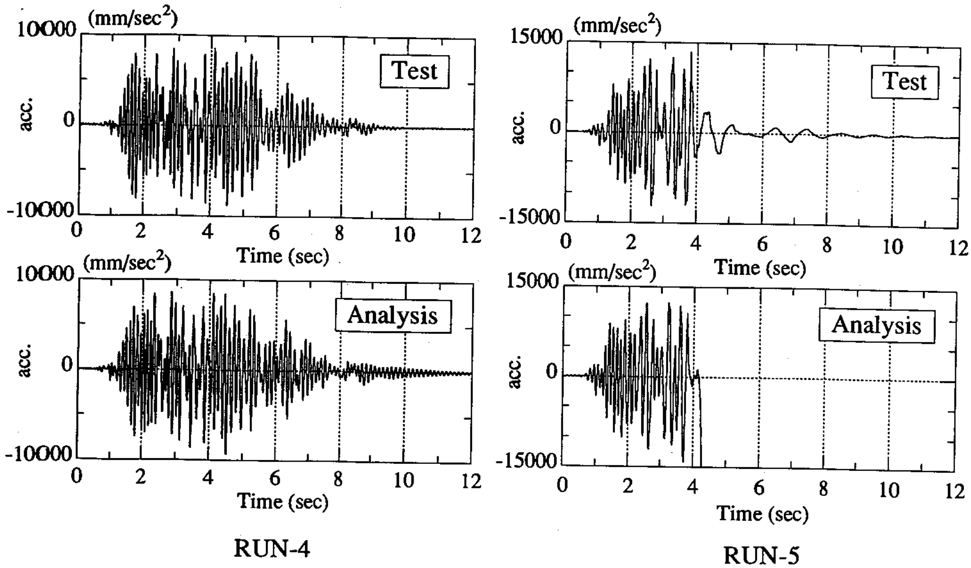

Fig.-12 Comparison of Analysis and Test on Response Acceleration

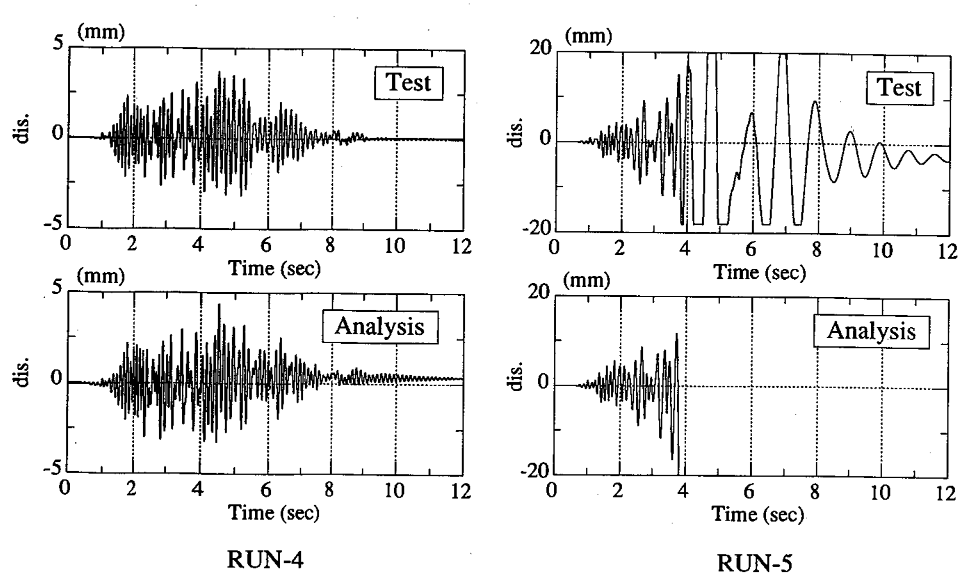

Fig.-13 Comparison of Analysis and Test on Response Displacement

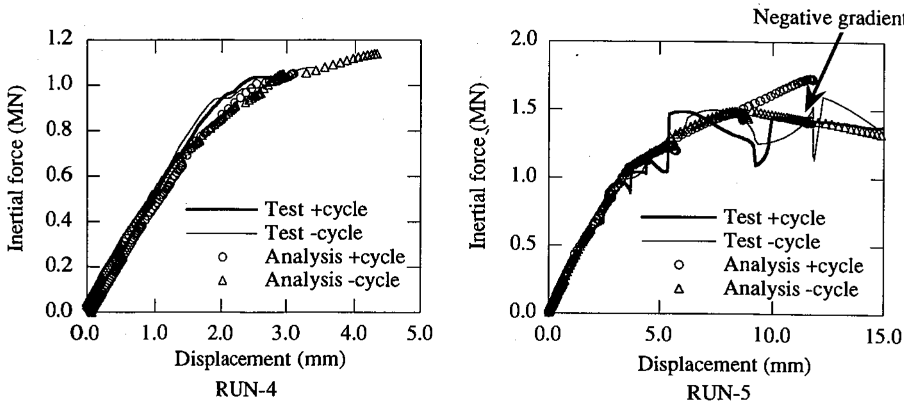

Fig.-14 Comparison of Analysis and Test on Envelope Curves

6. CONCLUSION

Using our original analytical method, the following items on the test could be simulated well.

- Inelastic response of acceleration and displacement time history before failure.
- The occurrence time of failure, by defining negative gradient of force-displacement relation in the analytical model.

7. REFERENCE

1. Kitada,Y., Akino, K., Aoyama, H. and Miller, A. : Report on seismic shear wall international standard problem organized by OECD/NEA/CSNI, *Transactions of the 14th SMiRT,* (to be published)

2. Nagashima, T., Shibata, A, Kanda, J., Igarashi, K., Akino, K., Taira, T. : Model test and inelastic analysis on dynamic response of RC shear walls , *Transactions of the 13th SMiRT,* Vol.3, pp.199-204

3. Ihzuka, T. and Noguchi, H. : Nonlinear Finite Element Analysis of Reinforced Concrete Members with Normal to High Strength Materials , *Proc. of JCI Annual Convention,* Vol.14, No.2 1992 (in Japanese)

4. Kupfer, H.B. and Gerstie, K.H. , : Behavior of Concrete Under Biaxial Stresses, *Journal of the Engineering Mechanics Division, Proceeding of the American Society of Civil Engineers,* Vol.99, No.EM4, pp.854-866, AUG., 1973.

5. Li, B., Maekawa, K. and Okamura, H. : Contact Density Model for Stress Transfer across Cracks in Concrete, *Jornal of the Faculty of Engineering, University of Tokyo (B),* Vol.40, No.1, pp.9-52, 1989

6. Miyatake, T. and Kubota, T. : Study on Reinforced Concrete Column (Part 1:Displacement at Rebar Yielding), *Transactions of the Architectual Insititute of Japan (Kanto branch)* Vol.37, 1966 pp.166-120 (in Japanese)